

Supplemental information

Neutrophil extracellular traps and DNases orchestrate formation of peritoneal adhesions

Julia Elrod, Annika Heuer, Jasmin Knopf, Janina Schoen, Lavinia Schönfeld, Magdalena Trochimiuk, Carolin Stiel, Birgit Appl, Laia Pagerols Raluy, Ceren Saygi, Leticija Zlatar, Sami Hosari, Dmytro Royzman, Thomas H. Winkler, Günter Lochnit, Moritz Leppkes, Robert Grützmann, Georg Schett, Christian Tomuschat, Konrad Reinshagen, Martin Herrmann, Tobias A. Fuchs, and Michael Boettcher

Supplement 1: Extracellular traps formation peaks at 72 hours after the induction of adhesions.

Time course of extracellular traps formation using Sytox orange staining of the peritoneal injury site. This supplemental Figure is related to Figure 1.

Supplement 2: Experimental design and treatment strategy of the murine models

(A) Experimental design of the adhesion model. Mice were subjected to a 1.5cm long peritoneal incision and two 6x0 Vicryl sutures. They were treated according to their group with either active or inactivated DNases. Experiments ended either after 72 hours (maximum of NET formation) or after 21 days (maximum of adhesion formation). Six groups were used for further experiments. In the treatment group mice received either 10 or 1mg/kg bodyweight Dornase alfa and NTR-10, respectively. This group was compared to shams (neither intervention nor treatment), to the control (received inactivated DNase1) and DNase1-knockout or *Dnase1/3*-knockout mice. This supplemental Figure is related to Figures 1-4.

Supplement 3: DNases affect neutrophil activation and NET formation in mice.

(A,G) Ly6G reflects the amount of neutrophil granulocytes. The DNases appear not directly to affect this parameter. (B-D,F-J) We assessed neutrophil extracellular traps and neutrophil activation by MPO, NE, and citH3 co-staining. The absence of DNASE1L3 (which reportedly is more tissue bound) significantly increased NETs deposition at the site of peritoneal injury. (J) Representative images of the triple staining: DNA-MPO-citH3. Data shown as mean±SD. Statistics: Kruskal-Wallis test with Dunn's correction. For more information on antibodies used, please refer to the STAR Methods section.

Supplement 4: Murine adhesions contain neutrophil elastase activity.

(A) Surgical sites from DNase1-KO, DNase1/3-KO, treated WT and WT mice show robust activity of neutrophil elastase (NE). (B) The NE activity of the surgical sites is resistant to the inhibition by the pharmacological inhibitor sivelestat and (C) the endogenous inhibitor α -1 antitrypsin (α 1-AT). For further information on proteins/peptides used, please refer to the STAR Methods section.

Supplement 5: The genes associated with NETs and/or neutrophils are differentially expressed after topical treatment with Dornase alfa.

Treatment with Dornase alfa mostly reduced immune response, leucocyte activation, NET formation and nucleosome assembly. (A) Volcano plot of 3718 significantly differentially expressed genes. 2875 of these genes are downregulated in murine peritoneal cavity cells after DNase1-treatment. (B,C) Volcano plots depicting genes associated with the GO terms regulation of leukocyte activation (B) and activation of immune response (C). Both termini are significantly enriched in DNase1-treated mouse peritoneal cavity cells. The top 20 most significant up and downregulated genes are labeled. (D) Volcano plots depicting previously described NET-associated genes (a) and marker genes of neutrophils (b) ²⁷. Genes that significantly differed in Dornase alfa versus mock-treated mouse peritoneal cavity cells are labeled. This supplemental Figure is related to Figures 3 and 4.

Supplement 6: Human adhesions contain NETs and DNase1/3.

Expression of the typical NET markers, neutrophil elastase (NE, green), citrullinated histone H3 (citH3, green) and myeloperoxidase (MPO, red) was detected in paraffin sections of surgically removed human adhesions (representative images shown). The presence of DNase1I3 (D1I3, green) was also shown in these adhesions. The enlarged details seen in the immunofluorescence staining and in the HE stained sections correspond to Figure 6. The specificity of all stainings was ensured by the negative signal in the isotype controls corresponding to the markers in the panel above the respective control. The size bar represents 50 μm (25 μm for Supplement 5 (3)). For more information on antibodies used, please refer to the STAR Methods section. This supplemental Figure is related to Figure 5.

Supplement 7: Human adhesions contain NET-borne proteins.

Presence of NET-borne proteins in human adhesions was validated by high-resolution mass spectrometry. As indicated the neutrophil proteins that are established to be bound to NETs like NE, MPO, Cathepsin G, S100-A8, and S100-A9 with high confidence. The secretory Proteinase3 was missing. This supplemental Figure is related to Figure 5.

Supplement 8: Human adhesions contain NETs and Fibrin.

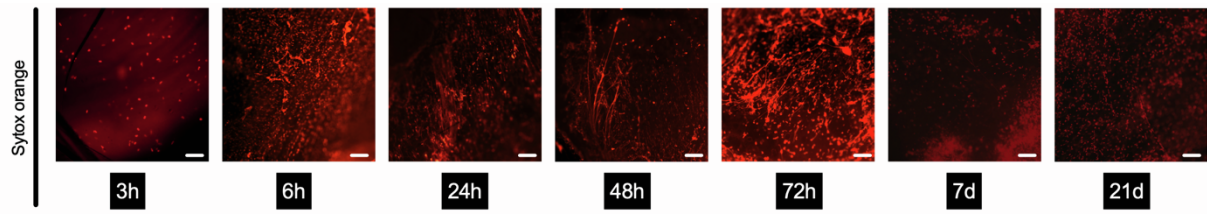
The classical NET markers anti-DNA, citrullinated H3 (citH3), and myeloperoxidase (MPO), all depicted in red, were detected by immunofluorescence staining of surgical specimens of human adhesions. Nuclei were stained by DAPI. The expression of the aforementioned NET markers co-localized with the detection of fibrin (red) in these tissue specimens. The specificity of all stainings was ensured by the negative signal in the isotype controls (wo1st) corresponding to the markers in the panel above the control. The size bar represents 500 μm . For more information on antibodies used, please refer to the STAR Methods section.

Supplement 9: The fibrin from human adhesions is post-translationally modified.

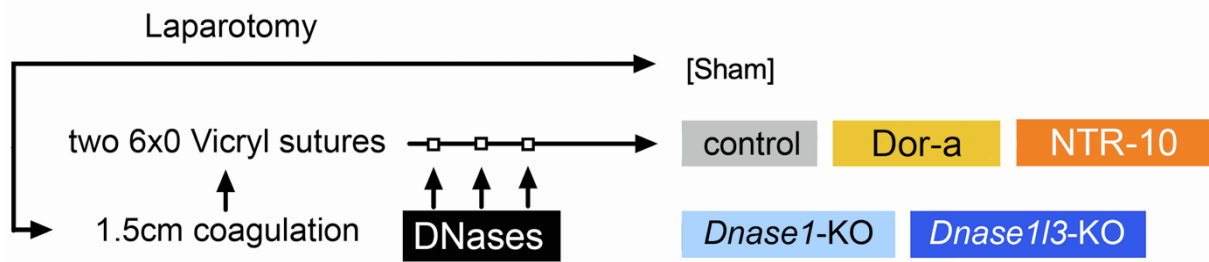
Analyses of the peptide sequences from mass spectrometry of human adhesions obtained by surgery also revealed many oxidized (ox, orange box), citrullinated (cit, yellow box), and carbamylated (Carb, grey box) peptides next to unmodified (w/o, blue box) ones in the alpha, beta and gamma chains of human fibrinogen. The thrombin cleavage site in the alpha chain is depicted in red, whereas the major plasmin cleavage sites in both chains are highlighted in green. * samples were fixed and subjected to antigen retrieval before mass spectrometry analyses. No major differences between fixed and unfixed samples were observed in the peptide analysis. This supplemental Figure is related to Figure 6.

Supplement 10: Plasmin(ogen) displays a lower Mascot score than fibrin and α 2-antiplasmin.

The abundance of fibrinolytic proteins in human adhesions was compared to fibrin by high-resolution mass spectrometry. Note, plasmin(ogen) displayed a much lower Mascot score than the fibrin chains in all samples. The inhibitory α 2-antiplasmin was higher than plasmin(ogen) and the plasmin activators tPA and uPA were absent in all but one sample. This supplement is related to Figure 6.

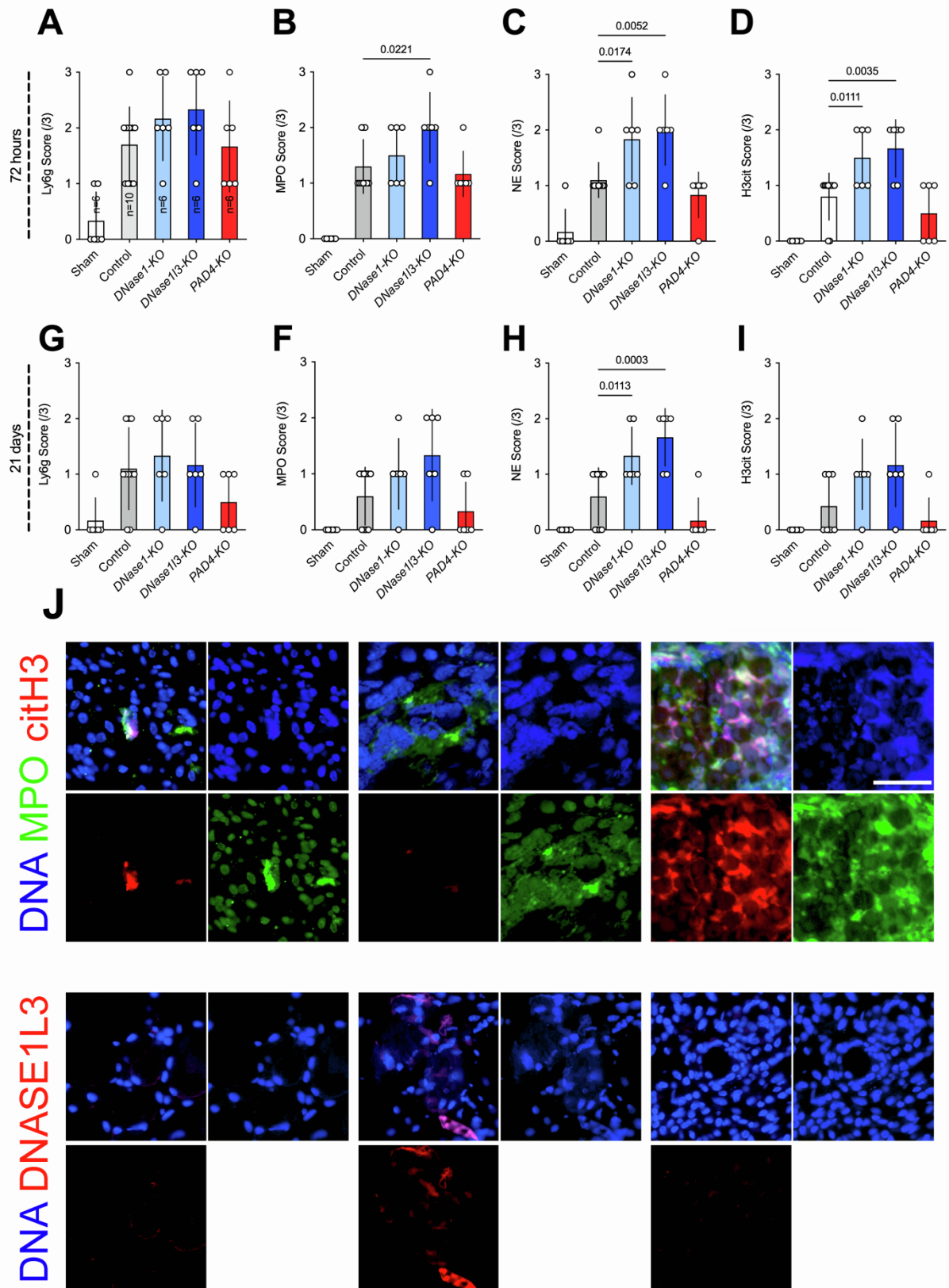


Supplement 1: Time course of extracellular DNA. A: Time course of extracellular traps formation using Sytox orange staining of the peritoneal injury site.



Supplement 2: Experimental design and treatment strategy of the murine models

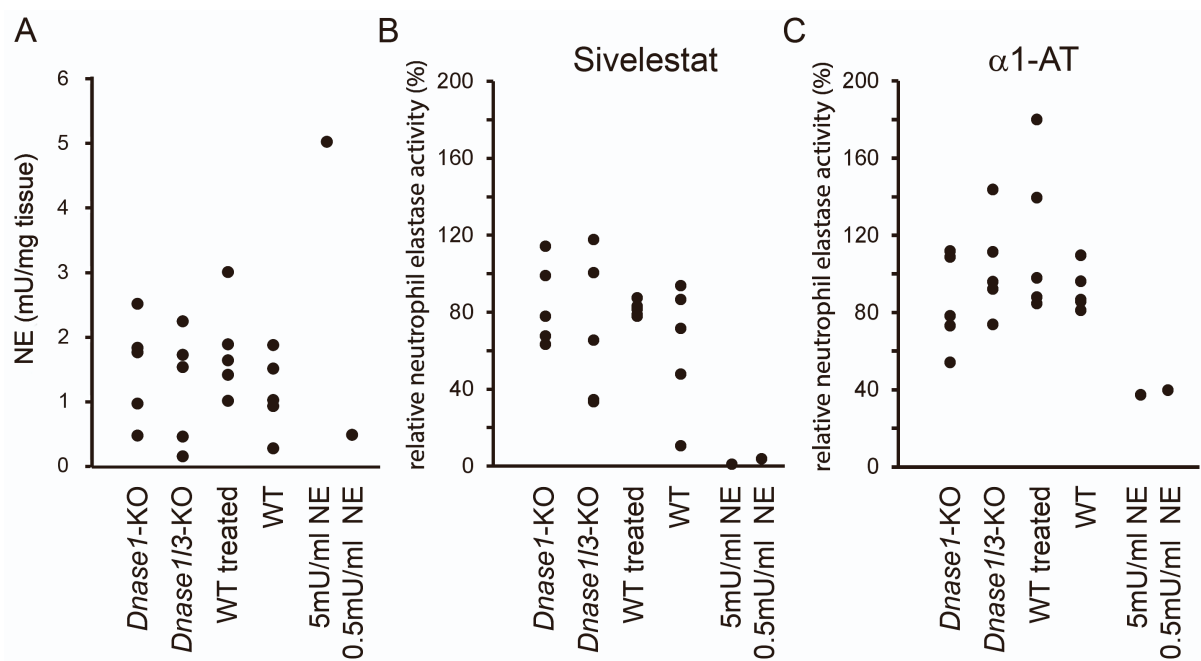
A: Experimental design of the adhesion model. Mice were subjected to a 1.5cm long peritoneal incision and two 6x0 Vicryl sutures. They were treated according to their group with either active or inactivated DNases. Experiments ended either after 72 hours (maximum of NET formation) or after 21 days (maximum of adhesion formation). Six groups were used for further experiments. In the treatment group mice received either 10 or 1mg/kg bodyweight Dornase alfa and NTR-10, respectively. This group was compared to shams (neither intervention nor treatment), to the control (received inactivated DNase1) and DNase1-knockout or *Dnase1I3*-knockout mice.



Supplement 3: DNases affect neutrophil activation and NET formation in mice.

(A,G) Ly6G reflects the amount of neutrophil granulocytes. The DNases appear not directly to affect this parameter. (B-D,F-J) We assessed neutrophil extracellular traps and neutrophil activation by MPO, NE, and citH3 co-staining. The absence of DNASE1L3 (which reportedly is more tissue bound) significantly

increased NETs deposition at the site of peritoneal injury. **(J)** Representative images of the triple staining: DNA-MPO-citH3. Data shown as mean \pm SD. Statistics: Kruskal-Wallis test with Dunn's correction.

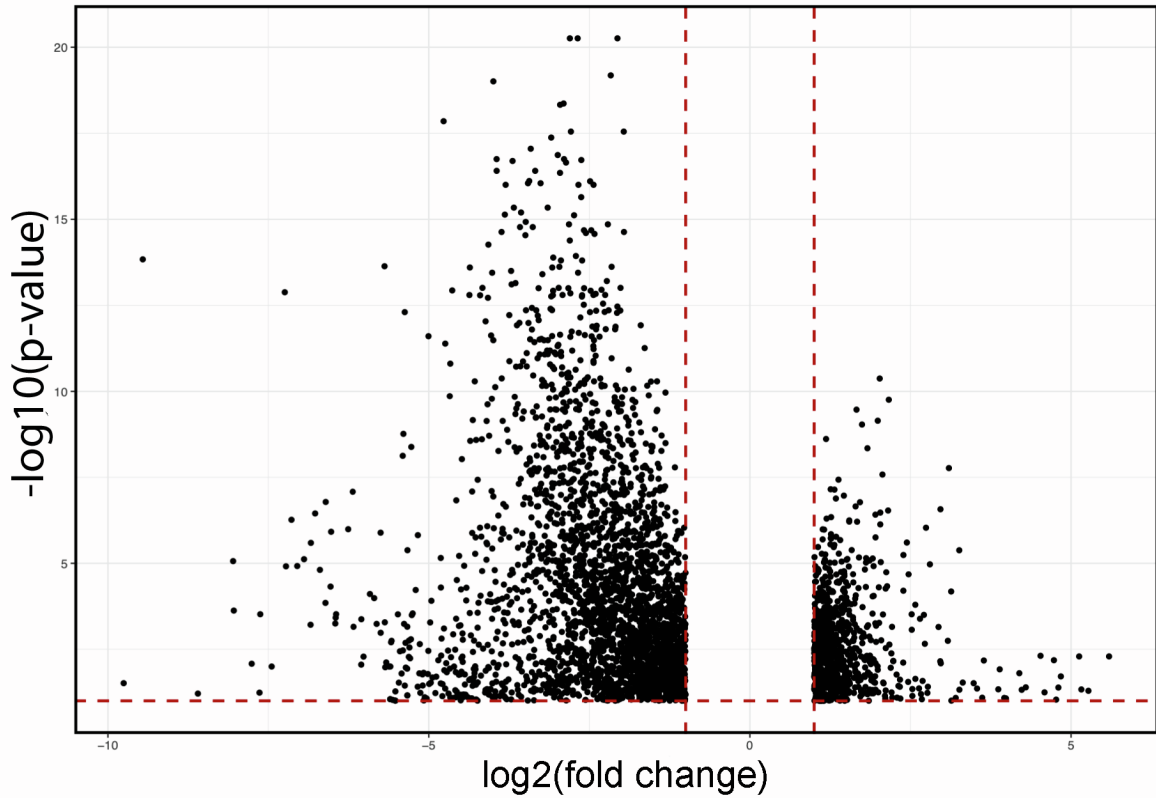


Supplement 4: Murine adhesions contain neutrophil elastase activity.

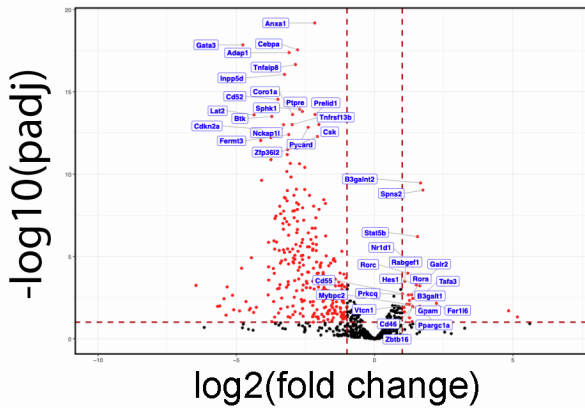
(A) Surgical sites from DNase1-KO, DNase1/3-KO, treated WT and WT mice show robust activity of neutrophil elastase (NE). (B) The NE activity of the surgical sites is resistant to the inhibition by the pharmacological inhibitor sivelestat and (C) the endogenous inhibitor α -1 antitrypsin (α 1-AT).

A

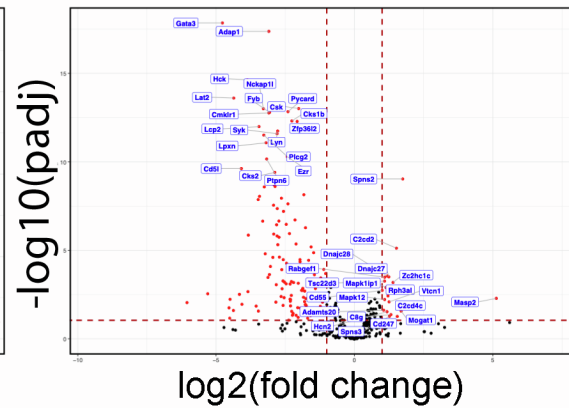
mock treated versus Dornase-alfa treated

**B**

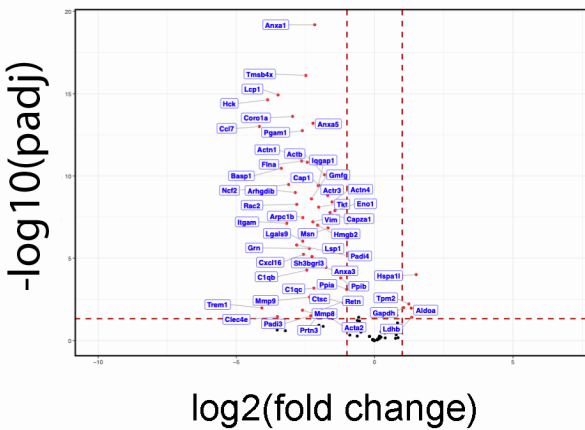
regulation of leucocyte adhesion

**C**

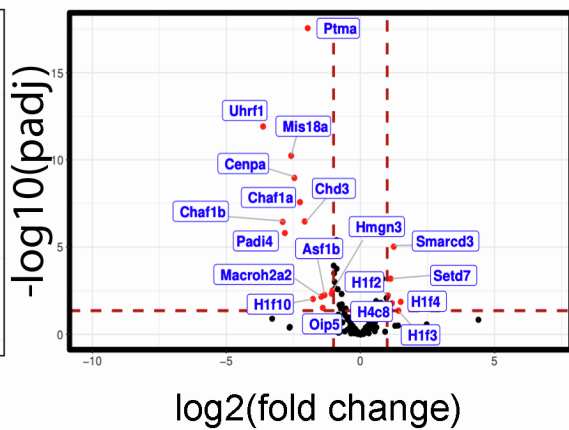
activation of immune response

**D**

NET-associated genes

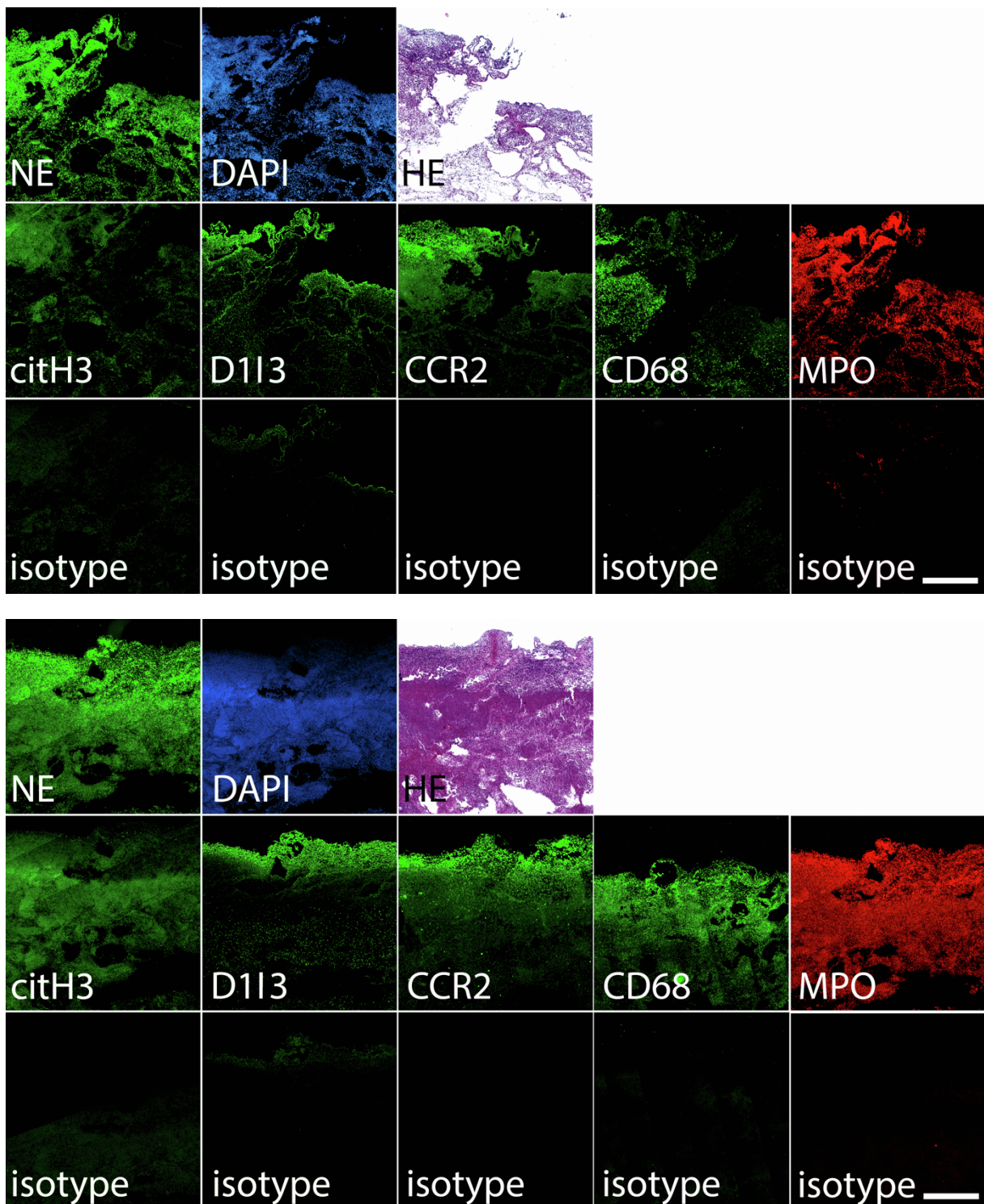
**E**

genes involved in nucleosome assembly (Reactome)



Supplement 5: The genes associated with NETs and/or neutrophils are differentially expressed after topical treatment with Dornase alfa.

Treatment with Dornase alfa mostly reduced immune response, leucocyte activation, NET formation and nucleosome assembly. (A) Volcano plot of 3718 significantly differentially expressed genes. 2875 of these genes are downregulated in murine peritoneal cavity cells after DNase1-treatment. (B,C) Volcano plots depicting genes associated with the GO terms regulation of leukocyte activation (B) and activation of immune response (C). Both termini are significantly enriched in DNase1-treated mouse peritoneal cavity cells. The top 20 most significant up and downregulated genes are labeled. (D) Volcano plots depicting previously described NET-associated genes (a) and marker genes of neutrophils (b) ²⁷. Genes that significantly differed in Dornase alfa versus mock-treated mouse peritoneal cavity cells are labeled.



Supplement 6: Human adhesions contain NETs and DNase113.

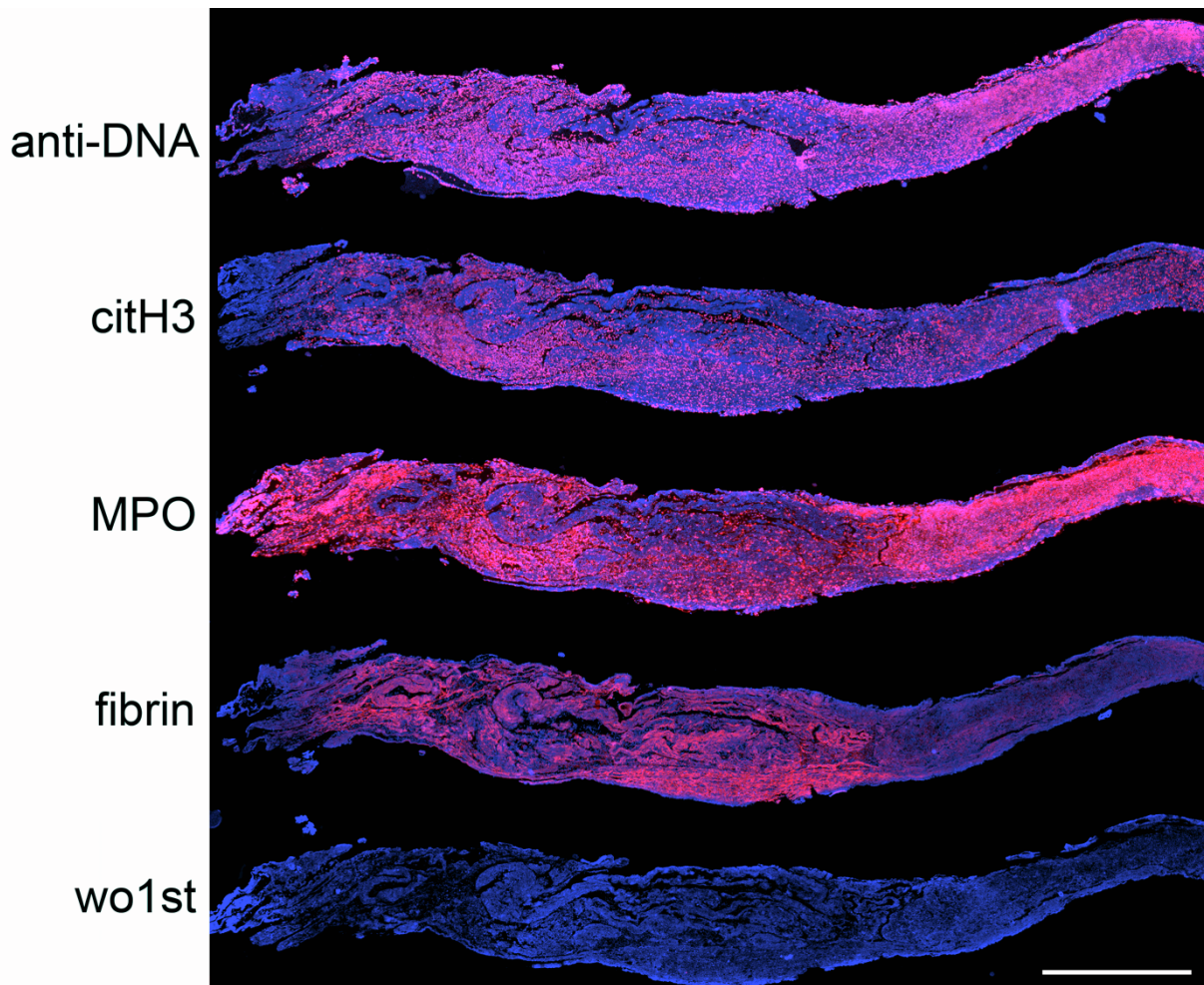
(A,B) Expression of the typical NET markers, neutrophil elastase (NE, green), citrullinated histone H3 (citH3, green) and myeloperoxidase (MPO, red) was detected in paraffin sections of surgically removed human adhesions (representative images shown). The presence of DNase113 (D113, green) was also shown in these adhesions. The enlarged details seen in the immunofluorescence staining and in the HE stained sections correspond to Figure 6. The specificity of all stainings was ensured by the negative

signal in the isotype controls corresponding to the markers in the panel above the respective control.
The size bar represents 50 μm (25 μm for Supplement 5 (3)).

Sample ID	Protein	Coverage [%]	Peptide count	PSMs	Unique Peptides	Amino acid count	MW [kDa]	calc. pI	Score Mascot
A-MB1	NE	42	8	51	8	267	28,5	9,35	1399
A-MB1	MPO	52	35	133	31	745	83,8	8,97	3887
A-MB1	Cathepsin G	50	13	40	13	255	28,8	11,19	1032
A-MB1	S100-A8	94	12	225	12	93	10,8	7,03	4340
A-MB1	S100-A9	96	11	508	11	114	13,2	6,13	7329
A-MB1	Proteinase 3								N.D.
A-MB2	NE	36	6	19	6	267	28,5	9,35	623
A-MB2	MPO	44	29	164	25	745	83,8	8,97	2983
A-MB2	Cathepsin G	36	10	20	10	255	28,8	11,19	268
A-MB2	S100-A8	81	10	97	10	93	10,8	7,03	1779
A-MB2	S100-A9	90	11	290	11	114	13,2	6,13	5427
A-MB2	Proteinase 3								N.D.
A-MB3	NE	44	8	55	8	267	28,5	9,35	1439
A-MB3	MPO	60	42	278	38	777	87,2	9,07	7078
A-MB3	Cathepsin G	51	15	57	15	255	28,8	11,19	1348
A-MB3	S100-A8	77	10	280	10	93	10,8	7,03	4704
A-MB3	S100-A9	93	13	631	13	114	13,2	6,13	8321
A-MB3	Proteinase 3								N.D.
A-MB4	NE								N.D.
A-MB4	MPO	17	6	7	6	745	83,8	8,97	27
A-MB4	Cathepsin G	56	13	29	13	255	28,8	11,19	580
A-MB4	S100-A8	32	3	4	3	93	10,8	7,03	117
A-MB4	S100-A9	85	8	20	8	114	13,2	6,13	321
A-MB4	Proteinase 3								N.D.
A-SH1	NE	42	9	43	9	267	28,5	9,35	847
A-SH1	MPO	50	43	279	38	745	83,8	8,97	5335
A-SH1	Cathepsin G	60	17	97	17	255	28,8	11,19	1802
A-SH1	S100-A8	100	21	583	21	93	10,8	7,03	8730
A-SH1	S100-A9	86	14	667	14	114	13,2	6,13	11315
A-SH1	Proteinase 3								N.D.
A-SH2	NE	54	7	10	7	267	28,5	9,35	203
A-SH2	MPO	49	34	56	30	745	83,8	8,97	745

Supplement 7: Human adhesions contain NET-borne proteins.

Presence of NET-borne proteins in human adhesions was validated by high-resolution mass spectrometry. As indicated the neutrophil proteins that are established to be bound to NETs like NE, MPO, Cathepsin G, S100-A8, and S100-A9 with high confidence. The secretory Proteinase3 was missing.



Supplement 8: Human adhesions contain NETs and Fibrin.

(A) The classical NET markers anti-DNA, citrullinated H3 (citH3), and myeloperoxidase (MPO), all depicted in red, were detected by immunofluorescence staining of surgical specimens of human adhesions. Nuclei were stained by DAPI. The expression of the aforementioned NET markers colocalized with the detection of fibrin (red) in these tissue specimens. The specificity of all stainings was ensured by the negative signal in the isotype controls (wo1st) corresponding to the markers in the panel above the control. The size bar represents 500 μm .

Supplement 9: The fibrin from human adhesions is post-translationally modified.

(A) Analyses of the peptide sequences from mass spectrometry of human adhesions obtained by surgery also revealed many oxidized (ox, orange box), citrullinated (cit, yellow box), and carbamylated (Carb, grey box) peptides next to unmodified (w/o, blue box) ones in the alpha, beta and gamma chains of human fibrinogen. The thrombin cleavage site in the alpha chain is depicted in red, whereas the major plasmin cleavage sites in both chains are highlighted in green. Samples were fixed and subjected to antigen retrieval before mass spectrometry analyses. No major differences between fixed and unfixed samples were observed in the peptide analysis.

Sample ID	Protein	Coverage [%]	Peptide count	PSMs	Unique Peptides	Amino acid count	MW [kDa]	calc. pI	Score Mascot
A-MB1	Fibrinogen a	51	41	242	41	866	94,9	6,01	5380
A-MB1	Fibrinogen b	77	39	315	39	491	55,9	8,27	9678
A-MB1	Fibrinogen g	76	32	199	6	453	51,5	5,62	5542
A-MB1	a2AP	49	18	42	18	491	54,5	6,29	1452
A-MB1	Plasminogen	67	40	98	30	810	90,5	7,24	2014
A-MB1	uPA-R	21	2	2	2	185	20,7	6,6	94
A-MB1	PAI1								N.D.
A-MB1	PAI2								N.D.
A-MB1	tPA								N.D.
A-MB1	uPA								N.D.
A-MB2	Fibrinogen a	49	42	166	25	866	94,9	6,01	3743
A-MB2	Fibrinogen b	75	45	224	45	491	55,9	8,27	6536
A-MB2	Fibrinogen g	62	25	115	4	445	50,3	6,09	3397
A-MB2	a2AP	27	11	20	11	491	54,5	6,29	559
A-MB2	Plasminogen	30	18	22	14	810	90,5	7,24	324
A-MB2	uPA-R	32	6	6	1	335	37	6,65	112
A-MB2	PAI1								N.D.
A-MB2	PAI2	47	13	18	7	415	46,6	5,63	398
A-MB2	tPA								N.D.
A-MB2	uPA								N.D.
A-MB3	Fibrinogen a	56	60	687	36	866	94,9	6,01	14030
A-MB3	Fibrinogen b	79	49	683	49	491	55,9	8,27	22196
A-MB3	Fibrinogen g	80	35	506	5	453	51,5	5,62	12472
A-MB3	a2AP	42	18	65	18	491	54,5	6,29	1784
A-MB3	Plasminogen	67	42	128	20	810	90,5	7,24	3040
A-MB3	uPA-R	22	5	5	5	335	37	6,65	196
A-MB3	PAI1								N.D.
A-MB3	PAI2								N.D.
A-MB3	tPA								N.D.
A-MB3	uPA								N.D.
A-MB4	Fibrinogen a	33	25	69	25	866	94,9	6,01	1198
A-MB4	Fibrinogen b	63	27	61	27	491	55,9	8,27	1815
A-MB4	Fibrinogen g	57	22	58	22	445	50,3	6,09	1642
A-MB4	a2AP	24	8	11	8	491	54,5	6,29	337
A-MB4	Plasminogen	14	6	7	3	810	90,5	7,24	184

A-SH8	PAI2	N.D.
A-SH8	tPA	N.D.
A-SH8	uPA	N.D.

Supplement 10: The plasminogen activators are virtually absent at adhesion site.

The abundance of fibrinolytic proteins in human adhesions was compared to fibrin by high-resolution mass spectrometry. Note, plasmin(ogen) displayed a much lower Mascot score than the fibrin chains in all samples. The inhibitory α 2-antiplasmin was higher than plasmin(ogen) and the plasmin activators tPA and uPA were absent in all but one sample.